

RESEARCH ARTICLE



Household Climate Resilience Index and Its Determinants: An Empirical Study in DKI Jakarta

Marta Sundari^a, Kusman Sadik^a, Aji Hamim Wigena^a, Anwar Fitrianto^a, Rizaldi Boer^{bc}

^a Statistics and Data Science, School of Data Science, Mathematics, and Informatics, IPB University, IPB Dramaga Campus, Bogor, 16680, Indonesia

^b Department of Meteorology and Geophysic, Faculty of Mathematics and Natural Sciences, IPB University, IPB Dramaga Campus, Bogor, 16680, Indonesia

^c Center for Climate Risk and Opportunity Management in Southeast Asia and Pacific, IPB University, IPB Dramaga Campus, Bogor, 16680, Indonesia

Article History

Received

11 September 2025

Revised 2 February 2026

Accepted 4 February 2026

Keywords

climate change, household resilience, robust principal component analysis, urban adaptation vulnerability



ABSTRACT

Climate change has intensified environmental pressures in urban coastal areas, particularly in DKI Jakarta, where recurrent flooding, tidal inundation, and heat extremes threaten urban sustainability. This study developed a Household Climate Resilience Index (HCRI) to assess the resilience of urban households to climate-related hazards using a robust principal analysis (RPCA) framework. The analysis was based on household survey data from 221 respondents across 17 urban villages in Jakarta, encompassing four resilience dimensions: exposure, sensitivity, incremental adaptation, and transformational adaptation. RPCA with a minimum covariance determinant estimator was applied to minimize the influence of outliers and ensure stable component estimation. The results reveal clear spatial heterogeneity in resilience, characterized by a distinct north–south gradient: northern coastal areas such as Kamal, Koja, and Pluit show the lowest resilience due to high flood exposure and land subsidence, whereas central and southern areas exhibit stronger adaptive capacity. The key determinants of resilience include flood frequency, household education levels, per-family expenditure, and proactive adaptation behaviors. The Kendall correlation test ($\tau = 0.518$, $p = 0.015$) confirmed a significant positive association between flood occurrence and low resilience levels. The developed HCRI provides a robust, data-driven framework to support targeted climate adaptation policies and urban resilience planning in Jakarta, Indonesia. HCRI outputs, together with the identified key determinants (flood frequency, education, per-family expenditure, and proactive adaptation), can guide the prioritization of urban environmental management and adaptation investments in the most vulnerable urban villages, including drainage upgrading, land subsidence control, and coastal protection.

Introduction

Climate change has intensified environmental pressures worldwide, as indicated by an approximate 1.1 °C increase in the global mean temperature relative to the pre-industrial era and the escalating frequency and intensity of extreme events, including floods, droughts, and sea-level rise [1–6]. In urban contexts, these hazards interact with long-standing stresses, such as ecosystem degradation, declining environmental quality, and service deficits, thereby weakening the ecological functions that support urban sustainability [7–9]. Coastal megacities are particularly exposed because risk is shaped not only by climatic forcing but also by the balance between environmental carrying capacity, infrastructure provision, and rapidly growing human demands, which together determine the magnitude and distribution of impacts [10,11]. Accordingly,

Corresponding Author: Marta Sundari  sundarimarta@apps.ipb.ac.id  Statistics and Data Science, School of Data Science, Mathematics, and Informatics, IPB University, IPB Dramaga Campus, Bogor, Indonesia.

© 2026 Sundari et al. This is an open-access article distributed under the terms of the Creative Commons Attribution (CC BY) license, allowing unrestricted use, distribution, and reproduction in any medium, provided proper credit is given to the original authors.

Think twice before printing this journal paper. Save paper, trees, and Earth!

strengthening adaptive capacity and resilience has become a strategic agenda for sustaining urban ecological functions and aligning development pathways with SDG 11 and 13 [3,6].

Resilience is widely recognized as a core lens for understanding how socio-ecological systems absorb disturbances, reorganize, and maintain essential functions during climate-related shocks [5,12]. In cities, resilience is multidimensional, integrating physical, social, economic, and institutional components, as well as the role of ecosystems and nature-based solutions in buffering hazards [7–9,13,14]. Because households represent the smallest socio-ecological unit, they experience hazards directly and respond through daily coping and adaptation, making household-scale evidence essential for assessing resilience in an operational and policy-relevant manner [15,16]. Importantly, household resilience in a coastal megacity is inseparable from the performance of urban environmental management systems, particularly drainage and pumping capacity, groundwater governance for land subsidence control, and coastal protection, because these systems shape the frequency, duration, and severity of hazards that households ultimately face [17–20].

In Indonesia, composite index approaches have been applied to assess urban climate resilience, including the Climate Disaster Resilience Index (CDRI) in Semarang [21]. Such work underscores that resilience emerges from the interaction between household resources and broader urban systems, including public services and governance [21]. However, DKI Jakarta faces a more complex risk environment: rapid urbanization coincides with land subsidence, seawater intrusion, and extreme rainfall, while socioeconomic inequality and dense informal settlements reinforce vulnerability and generate pronounced intra-urban heterogeneity [17–20]. These characteristics motivate household-based assessments as a necessary basis for identifying spatially heterogeneous resilience patterns and supporting targeted adaptation prioritization [16,22,23].

Despite the growing use of composite indices, two gaps remain salient in Indonesia's coastal megacities. First, many indices are operationalized at aggregated spatial scales that can mask intra-urban variation in exposure and adaptive capacity, thereby limiting policy targeting [9,15]. Second, indicator-weighting schemes are frequently sensitive to non-normality and multivariate outliers, which are common in household and environmental datasets. Under such conditions, a small subset of extreme observations can rotate the principal directions and destabilize weights, with implications for inference and prioritization [24–26]. These challenges are especially consequential for Jakarta, where hazard exposure and socioeconomic distributions tend to be heterogeneous and heavy-tailed across space [6,13].

To address these gaps, this study developed and validated a Household Climate Resilience Index (HCRI) for DKI Jakarta using a four-dimensional framework comprising exposure, sensitivity, incremental adaptation, and transformational adaptation [27]. To reduce the subjectivity associated with expert judgment weighting, we employed a reproducible, data-driven weighting approach based on a multivariate structure [27,28]. Specifically, the index is constructed using robust principal component analysis (RPCA), in which the location vector and covariance matrix are estimated robustly (e.g., via Minimum Covariance Determinant/ MCD-type estimators) so that component extraction and indicator weights are less sensitive to multivariate contamination than classical covariance-based PCA (principal component analysis) [24,29,30]. In addition, robustness considerations are addressed through sensitivity checks that examine whether key HCRI (Household Climate Resilience Index) patterns and determinant relationships remain stable under reasonable alternative specifications [24,30]. From an urban environmental management perspective, the HCRI is intended to translate household-level resilience evidence into actionable prioritization by linking resilience deficits to system-level levers, including drainage improvement, land subsidence control through groundwater governance, and coastal protection in highly exposed neighborhoods [6,18].

As an explicit scope limitation, this analysis focuses on mainland Jakarta and excludes island households; therefore, the findings and policy implications are intended to represent resilience dynamics in the urban mainland context rather than the distinct exposure profiles and governance conditions of island communities [18,27].

Materials and Methods

Study Area

Geographically, Jakarta lies between 5°19'12"–6°23'54" S and 106°22'42"–106°58'18" E, with an average elevation of 7 m above sea level. As shown in Figure 1, Jakarta, the capital city of Indonesia, covers 662.33 km² and consists of five municipalities and one regency, subdivided into 44 districts and 267 urban villages [31]. The city borders Depok, Bogor, and Bekasi to the south and east, Tangerang to the west, and the Java

Sea to the north of Jakarta. Situated on Java Island within the Pacific Ring of Fire, Jakarta is highly vulnerable to natural hazards such as flooding, land subsidence, and earthquakes, as well as non-natural risks, such as urban fires. The *Indeks Risiko Bencana Indonesia* (IRBI) in 2021 recorded a score of 60.43, classifying Jakarta as medium risk, with a declining trend since 2015, reflecting the city’s ongoing efforts to strengthen disaster resilience, infrastructure, and community preparedness [17].

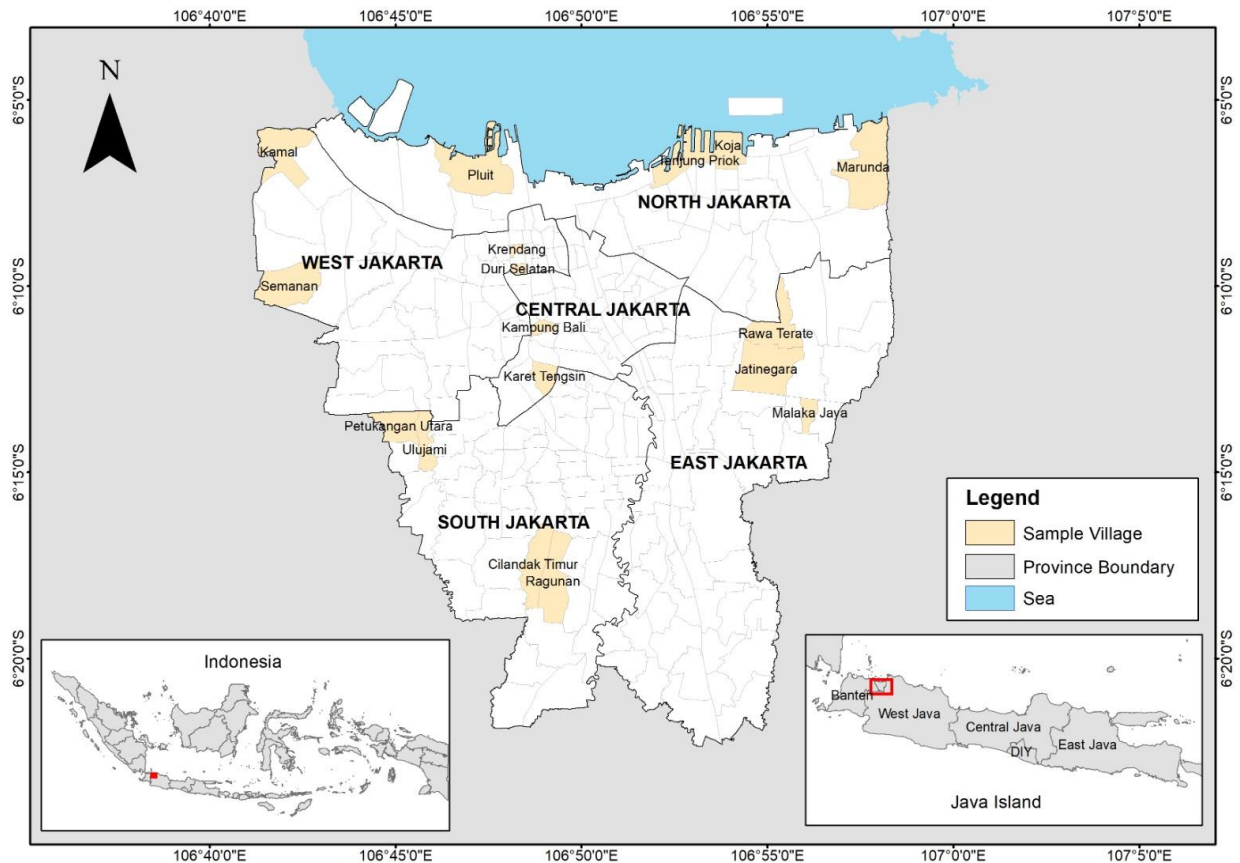


Figure 1. Study area and administrative boundaries of Jakarta, Indonesia. This map shows the Special Capital Region of Jakarta, including the five administrative municipalities (North, West, Central, East, and South Jakarta), with the sample villages highlighted in beige. Provincial boundaries and the adjacent sea are included to provide geographic and administrative context. The inset maps indicate the location of Jakarta within Java Island and Indonesia, emphasizing the spatial setting of the study area used in this research.

Data Collection Methods

The case study was conducted in DKI Jakarta, which comprises five municipalities with distinct climate risk profiles, ranging from highly vulnerable coastal areas in the north [18]. The HCRI was developed using household survey data on disaster risks related to climate change impacts, collected in 2022 by the Centre for Climate Risk and Opportunity Management in Southeast Asia and the Pacific (CCROM-SEAP), IPB University, in collaboration with *Dinas Lingkungan Hidup DKI Jakarta* (DLH DKI Jakarta). Urban villages were selected using an urgency-based vulnerability stratification derived from Jakarta’s multi-hazard climate risk profile (floods, droughts, tidal inundation, and extreme heat). This stratification was designed to ensure that the survey captured meaningful contrasts in the “exposure–sensitivity–adaptive capacity” framework that underpins the HCRI, so that sampled locations represent variation in hazard pressure (exposure), baseline fragility (sensitivity), and household coping/adjustment options (incremental and transformational adaptation). The urgency scenarios and vulnerability levels summarized in Tables 1 and 2 therefore function as the sampling frame to capture spatial heterogeneity in climate-related household resilience across municipalities, rather than as purely administrative descriptors.

Table 1. Distribution of urban villages across vulnerability levels under different urgency scenarios in Jakarta. This table presents the number of urban villages classified into vulnerability levels 1–7 for each urgency scenario, where each scenario represents a different combination of climate-related hazards, including flood, drought, tidal flood, and extreme heat. It also reports the total number of urban villages associated with each scenario, allowing comparison of how vulnerability is distributed across hazard combinations. Overall, most urban villages are concentrated in the intermediate vulnerability categories, particularly level 3, indicating that moderate vulnerability is more common than very high vulnerability across the study area.

No	Urgency	Type of urgency	Population							Number of urban villages		
			Vulnerability level									
			1	2	3	4	5	6	7			
1	1a	Flood Drought	Tidal flood						1	1		
2	1b	Flood Drought		Extreme heat		1	5	2		8		
3	1c	Flood		Tidal flood	Extreme heat				3	3		
4	2a	Flood Drought				2		1		3		
5	2b	Flood		Tidal flood		1	3	1		5		
6	2c	Flood			Extreme heat	2	8	5	3	1	19	
7	2d		Drought	Tidal flood					1	1		
8	2e		Drought		Extreme heat	5	1	1		7		
9	3a	Flood				2	9	6	6	2	25	
10	3b		Drought				1	1		2		
11	3c			Tidal flood		1		4	5	2	12	
12	3d				Extreme heat		13	20	5	1	39	
13	4-					8	31	54	31	9	3	136

Table 2. Distribution of selected urban villages across vulnerability levels in Jakarta. This table presents the selected sample urban villages and their classification across vulnerability levels 1–7 in the study area. Each urban village is placed under its corresponding vulnerability level, while the color scheme indicates its administrative municipality, namely West Jakarta, North Jakarta, South Jakarta, Central Jakarta, and East Jakarta. The table demonstrates that the selected samples represent multiple vulnerability categories and administrative areas, supporting the spatial and categorical diversity of the study sample.

No	Sample	Number of urban villages	Vulnerability level							
			1	2	3	4	5	6	7	
1	1								Koja	
2	1							Cilandak Timur		
3	1									Kamal
4	1								Rawa Terate	
5	1								Tanjung Priok	
6	2							Petukangan Utara		Semanan
7	1								Marunda	
8	1						Duri Selatan			
9	2				Karet Tensin					Jatinegara
10	1							Kampung Bali		
11	1				Pluit					
12	2				Ulujami		Krendang			
13	2		Ragunan	Malaka Jaya						

Legends:

West Jakarta	North Jakarta	South Jakarta	Central Jakarta	East Jakarta
--------------	---------------	---------------	-----------------	--------------

Jakarta's population reached 10,609,781 in 2021, with annual growth rate of 0.57%. It is the most densely populated province in Indonesia, with a population density of 15,978 persons per km² [32]. The household resilience survey was conducted in 2022. The survey sample was determined using Slovin's formula, using population 2.770.729 households and $e = 5\%$, the resulting sample comprised 400 respondents, comprising 221 mainland households, 26 island households, and 143 business units from 17 mainland and 4 island villages [33]. For the analytical model in this paper, we restricted the unit of analysis to 221 mainland households to (i) maintain a consistent household-based resilience construct (excluding business units with different exposure and decision logics) and (ii) ensure spatial feasibility for localized multivariate estimation, where each location requires a sufficient number of neighboring observations to form a stable geographically weighted covariance structure. This study focuses on 221 mainland households to ensure a sufficient number of neighbors for geographically weighted principal component analysis (GWPCA) in future research. Respondents represented three income groups—lower-middle, middle, and upper-middle—to capture income-based heterogeneity in the climate change impacts. This mainland focus also implies a scope limitation: the resulting HCRI patterns are intended to represent resilience dynamics in urban mainland Jakarta, while island households—whose exposure pathways and governance contexts differ—are not generalized from this analysis.

Survey Instruments and Field Procedures

Data were collected through structured face-to-face interviews using a final household questionnaire [33]. Household locations were recorded as X–Y–Z coordinates using the GPS Essentials application on a mobile phone. The instrument was organized into sequential modules covering (A) household sociodemographic characteristics; (B) housing conditions, including enumerator-based observation of building characteristics and on-site measurement of building and land area (length × width); (C–E) flood experience, adaptation responses, and flood impacts; and (F) flood exposure/potential flood damage measured with a building tape (e.g., house elevation relative to street and permanent doorstep barrier height). The questionnaire uses mixed response formats (binary, ordinal, and continuous entries in physical units and monetary values) and includes explicit skip instructions and multi-response items, which improves field consistency and enables replication. Enumerators received structured training not only on the questionnaire content and coding rules but also on field implementation procedures, including trial interviews to standardize probing, skip-pattern execution, and the measurement/observation components of the instrument.

Pre-Processing Data

Before the analysis, data preprocessing was performed in two stages. First, because the questionnaire produced both numerical and categorical measures, whereas classical PCA can be applied only to numerical data, ordinal categorical items were transformed to an interval scale using the method of successive intervals (MSI) [34]. This procedure yields continuous scores that preserve the rank order of the original responses and make the variables compatible with PCA. The MSI transformation was applied consistently across all ordinal indicators so that the subsequent covariance estimation reflected comparable measurement scales rather than mixed-scale artifacts. Second, multivariate outliers were diagnosed using a robust Mahalanobis distance [26]. Observations with distances exceeding a reference threshold, for example, the quantile of the chi-squared distribution with degrees of freedom equal to the number of variables, were flagged for further review prior to PCA. Importantly, flagged observations were not mechanically deleted; instead, outlier screening was used to motivate robust covariance estimation so that component directions were not dominated by a minority of extreme multivariate profiles, while households remained available for scoring and spatial mapping. These steps aimed to reduce the influence of extreme observations on the covariance estimation and principal component vectors, thereby improving the stability of the analysis.

Robust PCA Model Settings

This study adopts RPCA by estimating the location vector and covariance matrix using the MCD estimator, so that indicator weights are less sensitive to multivariate contamination than those obtained from classical covariance-based PCA. Conceptually, this choice is preferable to expert-based weighting when the objective is a reproducible, data-driven weighting scheme, and it is preferable to classical PCA when extreme observations can exert disproportionate leverage on the covariance structure and rotate the principal directions. PCA is commonly formulated for an $n \times p$ data matrix X , whose columns are the p observed variables. The first principal component is defined as the linear combination Xa that attains the maximum variance among all such combinations, where $\text{var}(Xa) = a'Sa$ and S is the sample covariance matrix. Under the unit-norm constraint $a'a = 1$, this maximization leads to the eigenvalue problem $Sa = \lambda a$: the loading

vector a is an eigenvector of S , and the corresponding eigenvalue λ equals the variance explained by that component; therefore, the first component corresponds to the largest eigenvalue λ_1 and its eigenvector a_1 [25]. Equivalently, PCA can be expressed through the singular value decomposition (SVD) of the column-centred data matrix X^* , where $(n - 1)S = X^{*'}X^*$; the right singular vectors of X^* coincide with the eigenvectors of S (the principal components loadings), and the component scores are obtained as X^*A , with component variances equal to squared singular values divided by $n - 1$ [25].

Technical Implementation

As shown in Figure 2, the HCRI was constructed through a sequential workflow consisting of indicator preparation, diagnostic screening, robust PCA estimation, and PC1-based index construction. RPCA was implemented in R using the `rrcov` package via covariance-based PCA with a robust scatter estimation. Principal components (PCs) were computed using `PcaCov(data,cov.control=CovControlMcd())`, where `CovControlMcd()` specifies the MCD estimator for the robust estimation of the location vector and covariance matrix used in the eigendecomposition. The resulting object was inspected using `summary(PcaCovMCD)` to obtain eigenvalues (variance explained), explained variance proportions, and the associated loadings and scores for index construction, with substantive emphasis placed on PC1 as the dominant one-number summary of joint variation across the indicator set [35].

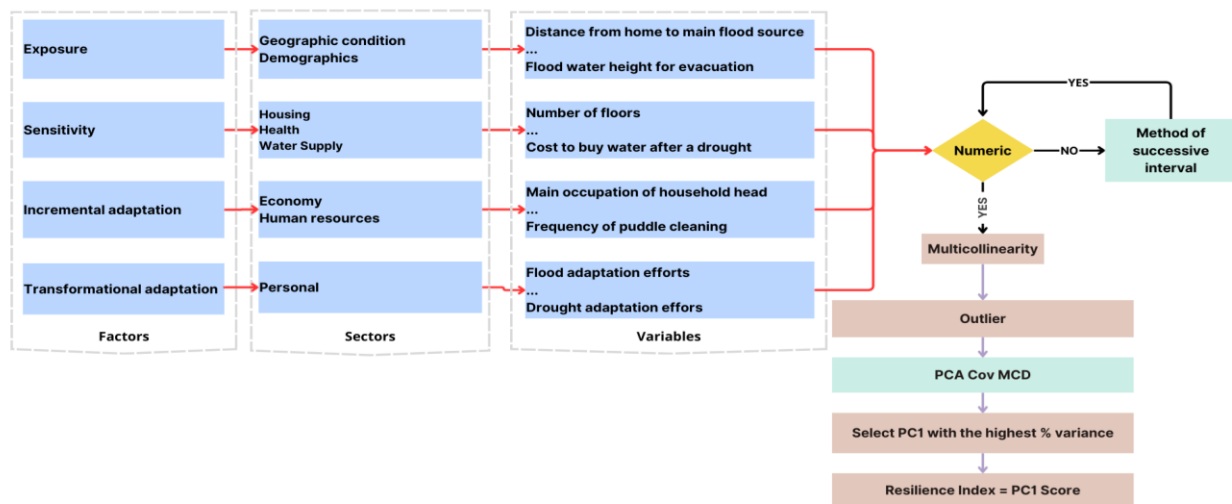


Figure 2. Workflow for constructing the HCRI using robust covariance-based PCA. This figure shows the steps used to develop the HCRI from factors, sectors, and observed variables. Numeric variables were screened for multicollinearity and outliers before applying robust PCA with the MCD estimator. The final index was defined using PC1 (first principal component), which explained the highest proportion of variance.

Household Climate Resilience Index Indicators

Resilience in socio-ecological systems is understood as the capacity to absorb shocks, maintain core functions, and adapt or transform in response to changes. It emphasizes the ability of social, economic, and environmental systems to withstand climate pressures and long-term disturbances while preserving their structure, identity, and essential functions and fostering learning and innovation [12,36]. Adaptive capacity is recognized as a key component of resilience and comprises four dimensions: exposure, sensitivity, incremental adaptive capacity, and transformational adaptive capacity [37]. Exposure reflects the degree to which a system is affected by climate risks, and sensitivity captures its internal vulnerability. The two forms of adaptive capacity represent a system's ability to implement gradual adjustments or fundamental structural changes to strengthen resilience against climate impacts [33,36].

Recent approaches have reinterpreted sensitivity as intrinsic resilience and exposure as non-exposure, both of which contribute positively to resilience. Together, these four dimensions complement each other in enhancing the overall resilience of socio-ecological systems [37]. To maintain conceptual consistency, each indicator in Table 3 was mapped a priori to one of the four resilience dimensions, and the hypothesized direction ("relatively resilient if...") reflects the expected sign of the indicator's contribution to resilience in the Jakarta coastal urban context. Indicators such as housing size/land area and flood-water height at

evacuation are interpreted through the mechanism they represent (baseline sensitivity versus hazard severity), and the hypothesized relationships are stated to make the index logic auditable and consistent with the socio-ecological framing of household resilience.

Table 3. Indicators used in constructing the HCRI. This table lists the indicators included in the HCRI, grouped by factor and sector, along with their codes, variable definitions, and hypothesized relationships with household resilience. The indicators cover key dimensions such as exposure and sensitivity, including geographical conditions, health, residence, and water sources. Overall, the table provides the conceptual basis for selecting and interpreting the variables used to measure household climate resilience in this study.

Indicator	Sector	Code	Variable	Hypothesized relationship: relatively resilient if:
Exposure	Geographical conditions	C2b	Distance of the house to the main flood source	A longer distance between the house and the primary disaster center is associated with a higher level of household resilience.
		C3b	Distance to other flood sources	A longer distance between the house and other disaster centers is associated with a higher level of household resilience.
		C4	(Invers) Amount of day flood in the past years	Measured by inverting the number of flood days per year; fewer flood events are associated with less frequent household exposure and higher resilience.
		F1	House elevation to street	A longer vertical distance of the house above road level is associated with a higher level of household resilience.
Health	Health	E11	(Invers) Proportion of sick family members after flood	A higher proportion of households that remain healthy after a flood is associated with greater household resilience.
		E14	Medication Expenditure	Higher expenditure on medicine after a disaster is associated with lower household resilience.
		I5	(Invers) Proportion of sick family members after drought	A higher proportion of households that remain healthy after a drought is associated with greater household resilience.
		N2	(Invers) Proportion of sick family with dengue	A higher proportion of households that remain healthy against dengue fever is associated with greater household resilience.
Sensitivity	Residence	B3	Building area	The wider the size of the house, the lower its resilience level.
		B4	Land area	The wider the size of the land, the lower its resilience level.
		B5	House building structure	Houses with permanent structures are associated with higher resilience.
	Residence	B6	Floor type	Houses with tiled floors are considered to have higher resilience compared to those with wooden floors.
		B7	Roof type	Houses with tiled roofs are considered to have higher resilience compared to those with zinc roofs.
		F2	Permanent dike height at main entrance	Dyke height is the inverse of house elevation relative to road level; thus, the lower the dyke, the higher the household resilience.
		F7	Flood water height for evacuation	The higher the water level at the time of evacuation, the higher the household resilience.
Sensitivity	Water sources	E9	Cost of buying water after a flood	Household expenditure on purchasing water reduces resilience.
		G1	Water Source for Toilet	Households that still rely on wells or rivers for sanitation needs are more sensitive compared to those using piped water supply (PDAM).
		G6	Water Source for drinking	Households that still rely on wells or rivers for food and drinking needs are more sensitive compared to those using piped water supply (PDAM).
		I3	Post-Drought Water Expenditure	Higher household expenditure on water during droughts is associated with a higher level of sensitivity.
Incremental Adaptation	Economics	A14	Expenses per family member	Household expenditure reflects household income; thus, higher expenditure is associated with greater adaptive capacity.
		A6	Main Occupation: Head of the family	The type of household head's occupation reflects their adaptive capacity. Household heads working as civil servants, military personnel, police officers, or in state-owned enterprises are considered to have higher adaptive capacity because their income is not disrupted during disasters.
		B2	Number of floors	The ability of a household to build houses with more than one floor indicates higher adaptive capacity, particularly in relation to flood disasters, thereby enhancing resilience.
	Human Resources	D3	Household Actions to Reduce Flood Loss	Represents adaptive efforts undertaken by households to reduce disaster-related losses.
		A4	Final education	Higher education levels of household heads are associated with greater household adaptive capacity.
		O2	Frequency of routine examination of mosquito larvae monitor officers	More frequent evaluations conducted by mosquito larvae monitor officers (<i>jumantik</i>) are considered to reflect higher household adaptive capacity in addressing potential disease outbreaks due to climate change.

Indicator	Sector	Code	Variable	Hypothesized relationship: relatively resilient if:
Incremental Adaptation	Human Resources	O3	Frequency of puddle cleaning	More frequent household cleaning activities are associated with greater adaptive capacity in reducing disaster-related health risks.
		D2	Flood Loss Mitigation Efforts	Household efforts to reduce the impacts of floods are associated with higher resilience.
	Personal	E4.1	Number of people cleaning the house	A higher number of household members involved in cleaning the house after a flood is associated with higher resilience.
		J2	Drought adaptation efforts	Household efforts to reduce the impacts of drought are associated with higher resilience.

Assessing Household Climate Resilience Index

Constructing a robust HCRI poses several methodological challenges. Subjective weighting methods, such as the analytic hierarchy process (AHP), are often biased [38]. To minimize subjectivity, data-driven techniques such as PCA are widely adopted; however, conventional PCA is highly sensitive to outliers, such as extreme flood or tidal inundation events. Therefore, this study employs RPCA with a MCD to obtain stable and reliable estimates [24,25,29,30].

PCA examines the associations among variables and simplifies complex datasets by transforming them into principal components (PCs), which are linear combinations that capture the maximum variance in the data. The variance proportion of each PC was calculated as the ratio of its eigenvalue to the total variance, with the cumulative explained variance serving as a criterion for PC selection. Typically, two to three PCs explaining at least 70% of the total variance are retained for interpretation, while trailing PCs may assist in outlier detection [38].

Robust PCA Outputs and HCRI Scoring Rule

In PCA, component loadings represent indicator weights, while scores represent the transformed coordinates of households in the component space [25]. The PC1 score is then used to construct the HCRI and classify households into five resilience categories based on quartile cut-offs and outlier boundaries, as presented in Table 4. The PC1 score is then used to form the index and classify households into resilience levels. The transformation of PC1 scores into resilience categories (extremely low to extremely high) is designed to support policy targeting and prioritization rather than to define an absolute “safe/unsafe” threshold. Because PCA-based indices are relative rankings that depend on the empirical distribution of the sample, quartile-based groupings are commonly used to translate continuous index scores into interpretable classes for mapping, communication, and program targeting [39,40].

Under this scheme, the low–high categories represent households below versus above the local distributional cut-points (Q_1 – Q_3), while extremely low/extremely high identify tail groups with atypical multivariate profiles that may require differentiated attention because disaster impacts and recovery constraints are often nonlinear and concentrated among the most vulnerable populations [41]. In practical terms, these classes enable an actionable “determinant → intervention” translation: exposure-dominant areas (e.g., frequent flooding) point to system-performance measures (drainage reliability, pumps, retention/pond management, and river–coastal interface management), sensitivity-driven deficits justify basic-service, housing, and health upgrades in the most exposed neighborhoods, and capacity-driven deficits motivate uptake support through preparedness financing, structured risk communication, and accessible institutional pathways—consistent with global guidance that effective adaptation requires coupling household actions with governance and infrastructure that reduce risk at scale [3,41].

Table 4. This table presents the transformation of PC1 scores into HCRI categories using score intervals and outlier boundaries. The lowest and highest extreme values are classified as extremely low and extremely high, while the remaining scores are grouped into very low, low, high, and very high. This classification serves as the basis for interpreting household resilience levels in the study.

Value range	HCRI transformation
Lower outlier	Extremely low
$< Q_1$	Very low
$Q_1 \leq \text{PC1 score} < Q_2$	Low
$Q_2 \leq \text{PC1 score} < Q_3$	High
$\geq Q_3$	Very high
Upper outlier	Extremely high

Results and Discussion

Results

Data Diagnostics and Justification for RPCA–MCD

The robust mahalanobis distance (RMD) analysis indicated that 95 observations exceeded the χ^2 (99%) cutoff of 27.688 ($p = 13$), classifying 41.6% of households as multivariate outliers (Figure 3). This proportion is substantial and signals that the joint indicator structure is heterogeneous; therefore, atypical households cannot be treated as marginal “noise” evaluated per indicator in isolation. This diagnostic motivates the use of RPCA rather than classical covariance-based PCA, because classical PCA can be rotated by a minority of leverage points that disproportionately affect the sample covariance matrix and thus the eigenvectors that define the principal directions [25,42].

Using RPCA with MCD-based covariance estimation, PC1 explained 87.38% of the total variance, exceeding the 70% threshold used for a parsimonious one-number index. In PCA terms, PC1 is a linear combination of indicators that maximizes the variance of the projected scores under a unit-norm constraint, which leads to the eigenvalue problem of the covariance matrix. In the robust setting, the same geometric logic applies, but the covariance matrix is replaced by a high-breakdown robust scatter estimate, making the resulting eigenstructure less sensitive to contamination [25,42]. Substantively, the high variance captured by PC1 supports its use as the dominant resilience gradient across households, but it should be interpreted as a multivariate “syndrome” of co-varying conditions, rather than a single-cause ranking.

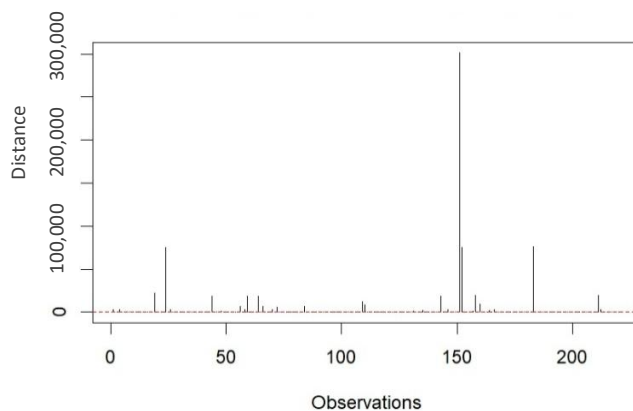


Figure 3. Robust mahalanobis distance values and outlier cutoff based on the MCD estimator. This figure displays the robust mahalanobis distance for each observation, with observations shown on the x-axis and distance values on the y-axis. The dashed horizontal line represents the 99% chi-square cutoff used to identify potential multivariate outliers. Observations exceeding this threshold are considered outliers, indicating cases that deviate substantially from the overall data structure.

Socio-Demographic Contrasts in Resilience Classes

The HCRI gradient should be interpreted as a coupled human–environment outcome in which household capacities (education, expenditure, and behaviors) interact with urban environmental management systems that shape hazard frequency and severity. In Jakarta, household resilience is structurally conditioned by flood control and drainage performance, land subsidence dynamics linked to groundwater governance, and coastal processes that can amplify compound flooding [43,44]. Therefore, the HCRI should be read not only as a socioeconomic capacity index but also as an indicator of how environmental services and infrastructure translate climate pressures into household-level exposure, sensitivity, and feasible adaptation pathways [45,46].

Figure 4 illustrates the relationship between education level and the HCRI. Respondents with higher education levels demonstrated stronger resilience, with 78.57% of university graduates classified in the very high–high category compared to 21.43% in the low–extremely low group. In contrast, resilience levels decline markedly among respondents with lower education levels: 64.52% of junior high school, 74.29% of elementary, and 88.89% of non-formal education respondents fall into the low–extremely low categories. These results indicate that educational attainment significantly shapes climate resilience. Individuals with

higher education are more likely to access climate-related information, understand adaptation programs, and make informed decisions in the face of environmental stress. Akter et al. [15] noted that education enhances household resilience by improving cognitive and behavioral responses to climate risks through greater awareness and the capacity to process information.

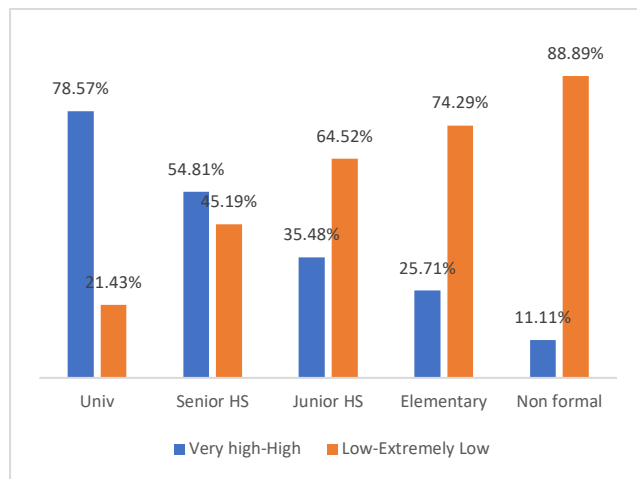


Figure 4. Distribution of HCRI categories by education level. This figure compares the proportion of households in the very high–high and low–extremely low resilience categories across different education levels. Higher education is associated with a greater share of households in the higher resilience category.

The distribution of respondents’ length of residence shows that 93.21% have lived in their current area for over ten years, indicating deep familiarity with local environmental conditions and hazards. Figure 5 confirms that those residing for more than 10 years display a balanced resilience profile (50.49% very high–high; 49.51% low–extremely low), while households with 5–10 years of residence show slightly weaker resilience (45.45% very high–high; 54.55% low–extremely low). This pattern suggests that long-term residence strengthens environmental awareness and collective preparedness, whereas newly settled populations may still be developing social capital and localized adaptive practices. These findings align with Matandirotya et al. [47], who reported that communities with extended environmental engagement, such as *vhaVenda* and *baTonga* in Southern Africa, build deep local knowledge that enhances early warning, resource management, and adaptive responses to climate variability.

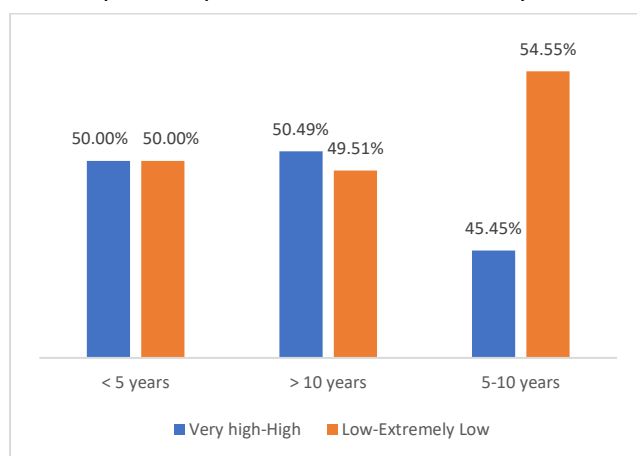


Figure 5. Distribution of HCRI categories by length of residence. This figure shows the proportion of respondents in the very high–high and low–extremely low resilience categories across three residence duration groups: < 5 years, 5–10 years, and > 10 years. The comparison indicates that resilience levels vary across residence duration, with those residing for more than 10 years showing a more balanced profile, while those with 5–10 years of residence show a higher proportion in the lower resilience category.

Employment status also influenced adaptive capacity and resilience distribution (Figure 6). Households with more stable or flexible income sources tend to be more resilient. Among respondents, 69.7% of unemployed households surprisingly fell into the very high–high resilience category, potentially reflecting strong informal social support networks and collective adaptation mechanisms. Conversely, only 42.86% of civil servants, 43.75% of SOE employees, and 49.32% of private sector employees demonstrated high resilience, suggesting that formal employment does not necessarily guarantee adaptive flexibility. Meanwhile, self-employed households exhibit a relatively balanced resilience profile (47.17% very high–high; 52.83% low–extremely low), highlighting the duality between income independence and vulnerability to economic shocks. This finding aligns with other studies who emphasized that livelihood diversification, job stability, and informal sector adaptability play crucial roles in shaping household resilience to climate-related risks in urban Asia [23,48].

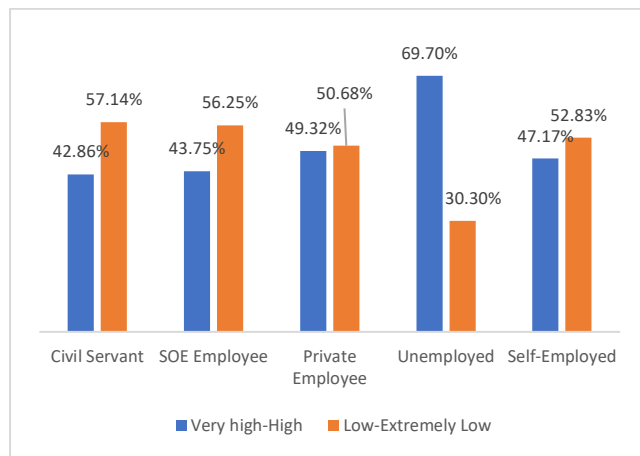


Figure 6. Distribution of HCRI categories by employment status. This figure shows the proportion of respondents in the very high–high and low–extremely low resilience categories across five employment groups: civil servants, SOE employees, private employees, unemployed, and self-employed respondents. The distribution indicates that resilience levels vary by employment status, with unemployed respondents having the highest proportion in the higher resilience category, while several other groups are more concentrated in the lower resilience category. These results suggest that employment status is associated with differences in household climate resilience.

Spatial Distribution of HCRI Across Administrative Cities and Urban Villages

The analysis of household resilience to climate change across the five administrative cities of DKI Jakarta, as presented in Table 5, revealed spatial variation influenced by the type of hazard and the level of regional vulnerability. West Jakarta showed a sharp contrast between areas with moderate and very high vulnerability. Duri Selatan and Krendang, classified as moderately vulnerable and primarily exposed to drought and heatwaves [33], demonstrate high resilience levels, with 84.6% and 69.2% of households, respectively, categorized as “high” to “very high”. This indicates that seasonal and predictable climate hazards, such as droughts and extreme temperatures, are easier for communities to anticipate. Conversely, Kamal and Semanan—both with very high vulnerability and frequently affected by floods and tidal inundation—display the lowest resilience. In Kamal, 84.6% of households fall into the “extremely low” category, while in Semanan, 53.9% are in the “low” category and 15.4% in the “very low” category.

Central Jakarta exhibited moderate-to-high resilience levels. Kampung Bali, despite having high vulnerability and exposure to drought, records 92.3% of households in the “high” and “very high” categories. In contrast, Karet Tengsin, with low vulnerability but prone to flooding, shows 61.5% of households in the “low” vulnerability category. This finding indicates that even areas with low vulnerability can have weak resilience when they are frequently affected by floods. South Jakarta has diverse resilience patterns. Cilandak Timur and Petukangan Utara, both highly vulnerable and facing multiple hazards such as floods, droughts, and extreme temperatures, display a relatively balanced distribution—38.5% of households fall into the “High” to “very high” categories, while another 38.5% are in the “very low” to “extremely low” categories. Meanwhile, Ragunan (very low vulnerability) and Ulujami (low vulnerability but exposed to extreme heat) showed more stable resilience, with 46.1% and 61.5% of households, respectively, in the “high” to “very high” categories.

Table 5. Classification of HCRI categories by urban village. This table presents the distribution of household climate resilience categories for each selected urban village, grouped by municipality in Jakarta. It also shows the corresponding vulnerability level and dominant disaster type for each urban village, together with the percentage of households classified into each resilience category, from “very high” to “extremely low”. Overall, the table highlights substantial variation in household resilience across urban villages and municipalities, indicating differences in local vulnerability and disaster exposure.

Urban city	Vulnerability	Disaster	Household climate resilience index (%)				
			Very high	High	Low	Very low	Extremely low
West Jakarta							
Duri Selatan	Moderate	Drought, Extreme heat	23.08	61.54	15.38		
Kamal	Extremely high	Flood, Tidal flood, Extreme heat	7.69	7.69			84.62
Krendang	Moderate	Extreme heat	46.15	23.08	15.38	7.69	7.69
Semanan	Extremely high	Flood, Extreme heat	7.69	15.38	53.85	15.38	7.69
Central Jakarta							
Kampung Bali	High	Drought	46.15	46.15	7.69		
Karet Tengsin	Low	Flood	7.69	30.77	61.54		
South Jakarta							
Cilandak Timur	High	Flood, Drought, Extreme heat	23.08	15.38	23.08	30.77	7.69
North Petukangan	High	Flood, Extreme heat	15.38	46.15	23.08		15.38
Ragunan	Extremely low		30.77	15.38	46.15		7.69
Ulujami	Low	Extreme heat	23.08	38.46	30.77		7.69
East Jakarta							
Jatinegara	Extremely high	Flood	46.15	53.85			
Malaka Jaya	Very low		53.85	30.77	7.69	7.69	
Rawa Terate	Very high	Flood, drought	15.38	7.69	38.46	23.08	15.38
North Jakarta							
Koja	Very high	Flood, drought, tidal flood	23.08	23.08	38.46	7.69	7.69
Marunda	Very high	Drought, tidal flood	46.15	7.69			46.15
Pluit	Low	Tidal flood	15.38		46.15	15.38	23.08
Tanjung Priok	Very high	Flood, tidal flood			15.38	61.54	23.08

East Jakarta has a relatively strong adaptive capacity despite facing significant climate hazards. Jatinegara, with very high vulnerability and flood risk, records 46.2% of households in the “very high” category and 53.8% in the “high” category. Malaka Jaya, which has very low vulnerability, also shows positive results, with 84.6% of households in the “high” to “very high” vulnerability categories. Conversely, Rawa Terate—with very high vulnerability and exposure to both floods and droughts—shows more varied results: 38.5% of households fall into the “low” category, 23.1% into “very low,” and 15.4% into “extremely low”.

North Jakarta experienced the highest climate stress and lowest resilience among all administrative cities. Koja, with very high vulnerability and exposure to floods, droughts, and tidal inundation, shows 46.1% of households in the “low” category and only 23.1% in the “high” category. Marunda displays a highly polarized pattern, with 46.2% of households in the “very high” and 46.2% in the “extremely low” categories, reflecting deep resilience inequality in the coastal zones. Pluit, with low vulnerability but frequent tidal flooding, shows 46.1% of households in the “low” category and 38.5% in the “very low” category. Meanwhile, Tanjung Priok—with very high vulnerability and exposure to floods and tidal inundation—records 61.5% of households in the “very low” category and 23.1% in the “extremely low” category. These findings emphasize that a combination of land subsidence, seawater intrusion, and structural poverty are the main causes of low adaptive capacity in the northern coastal areas.

Overall, the results highlight a clear north–south spatial gradient in household resilience. The northern coastal areas consistently exhibited lower resilience, whereas the southern and central regions demonstrated higher resilience. Hydrological hazards such as floods and tidal floods are strongly associated with lower resilience, over 60% of households fall into the “low” to “extremely low” categories whereas drought and extreme temperature hazards correlate with higher resilience, with more than 70% of households categorized as “high” to “very high”. These findings indicate that vulnerability levels do not always directly correspond to resilience outcomes. Figure 7 shows the spatial distribution of urban village vulnerability and Figure 8 presents the spatial distribution of household resilience across Jakarta.

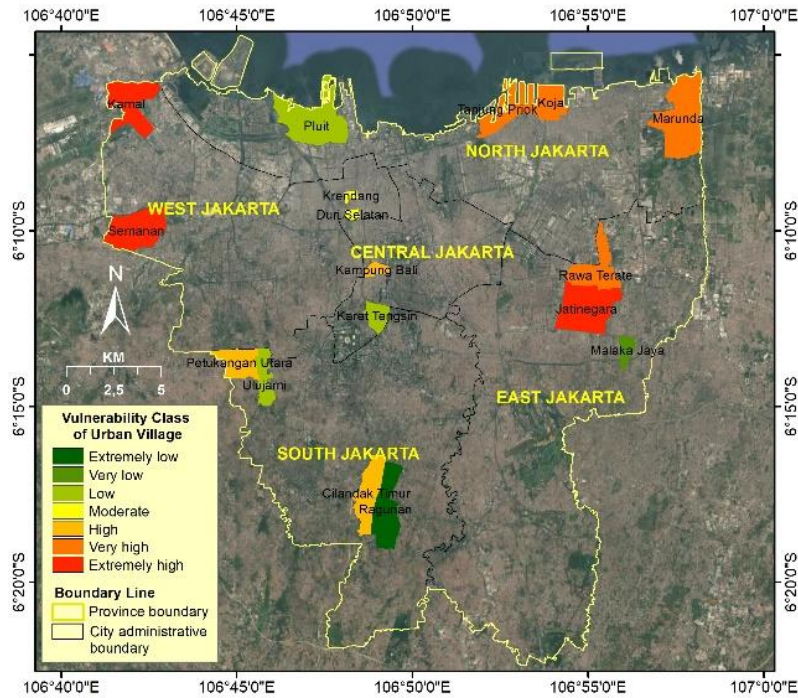


Figure 7. Spatial distribution of the Urban Village Vulnerability Index in Jakarta. This figure presents the vulnerability classes of the selected urban villages across Jakarta, displayed on a map with administrative and provincial boundaries. Each urban village is color-coded from extremely low to extremely high to show differences in vulnerability levels across the study area. The map highlights the spatial variation in urban village vulnerability and provides geographic context for interpreting local climate-related risk.

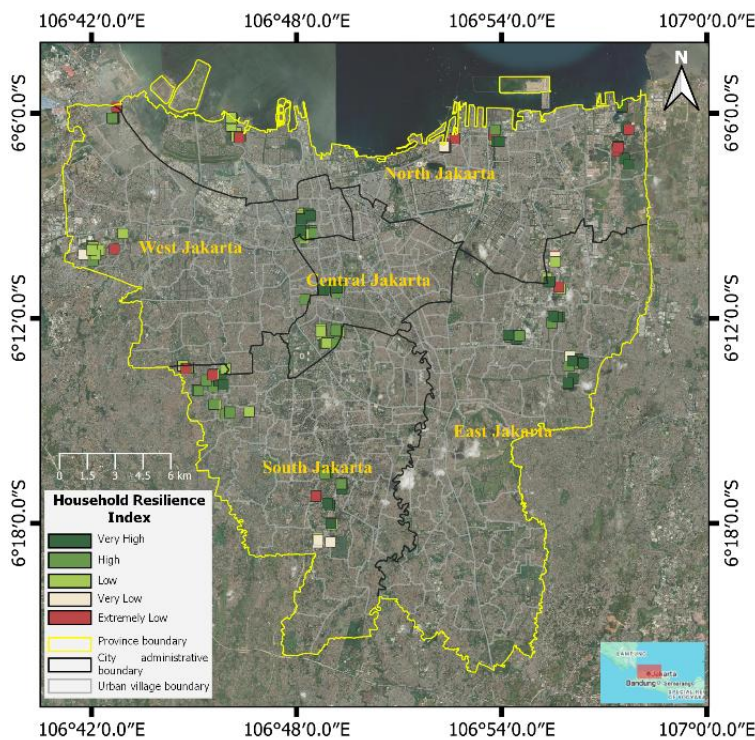


Figure 8. Spatial distribution of the Household Resilience Index (HRI) in Jakarta. This figure shows the distribution of household resilience categories across the study area, displayed on a map with urban village, administrative, and provincial boundaries. Household resilience is classified into five categories, ranging from extremely low to very high, to illustrate spatial differences in resilience levels. The map highlights the geographic variation in household resilience across Jakarta and supports the identification of areas with lower and higher resilience.

Discussion

Determinants of Resilience and Flood–Resilience Association

The Kendall correlation test result ($\tau = 0.518$, $p = 0.015$) indicates a positive and significant relationship between flood events and the proportion of households with low HCRI values. This confirms that areas affected by floods tend to have a higher proportion of low-resilience households than those not affected. Although the RPCA MCD approach effectively identifies the key determinants of resilience, it assumes spatial stationarity in the relationships across Jakarta. Considering the spatial heterogeneity between the northern coastal and southern inland areas, geographically weighted PCA (GWPCA) [49–52] was applied to capture local variations in indicator influence. This spatially adaptive approach provides a more detailed understanding of place-based resilience patterns in the DKI Jakarta area.

Several PCA-based loadings reported in this section are numerically small (e.g., < 0.01). This does not automatically imply “no effect” in substantive terms because loadings are scale-dependent and reflect how variables contribute to the variance-maximizing direction under the chosen preprocessing (centering/standardization) and covariance estimate. In particular, when indicators are standardized, a small loading indicates a weak contribution to the dominant co-variation pattern captured by PC1, not necessarily irrelevant to household welfare or policy design. Conversely, a very large loading (e.g., flood frequency ≈ 0.999) indicates that the exposure gradient is overwhelmingly structured by the indicator within the extracted component. Therefore, interpretation should focus on (i) relative magnitude within the same PCA run and (ii) sign/direction of association. Practically, indicators with consistently near-zero loadings can be treated as secondary for explaining PC1, while still remaining relevant for targeted sectoral programs outside the one-number index. This empirical pattern also provides a clear methodological motivation for future work toward sparse–robust GWPCA: when many indicators contribute weakly to the dominant component, sparsity-inducing penalties (e.g., elastic net) within a geographically weighted, robust covariance framework can formalize variable selection by shrinking negligible local loadings toward zero, while retaining the most informative indicators that consistently shape PC1 across locations. A sparse–robust GWPCA would therefore improve interpretability and policy communication by identifying a parsimonious, place-specific subset of determinants, while robustification maintains stability under outliers and heterogeneous urban households.

The HCRI gradient should be interpreted as a coupled human–environment outcome in which household capacities (education, expenditure, and behaviors) interact with urban environmental management systems that shape hazard frequency and severity. In Jakarta, household resilience is structurally conditioned by flood control and drainage performance, land subsidence dynamics linked to groundwater governance, and coastal processes that can amplify compound flooding [43,44]. Therefore, the HCRI should be read not only as a socioeconomic capacity index but also as an indicator of how environmental services and infrastructure translate climate pressures into household-level exposure, sensitivity, and feasible adaptation pathways [45,46].

As shown in Figure 9, the PCA results for the exposure indicator, the variables “frequency of floods in the past years (C4)” and “house elevation to street (F1)” showed the highest loading values, at 0.9993 and 0.0121, respectively. These results indicate that flood frequency is the most dominant factor explaining household exposure to climate hazards, whereas house elevation plays a minor but relevant role in reducing direct exposure. Areas that experience frequent flooding—such as Kamal, Semanan, Koja, and Pluit—tend to have higher exposure levels and a larger proportion of households with low HCRI values, reflecting limited adaptive capacity. Conversely, a higher house elevation provides a form of physical protection that can slightly mitigate exposure, although its influence remains relatively small compared to the strong impact of flood frequency on reducing household resilience to climate change in DKI Jakarta.

Regarding exposure, the PCA results showed that flood frequency in recent years (C4) had the highest loading (0.9993), whereas house elevation relative to the street (F1) had a much smaller loading (0.0121). This implies that recurrent flooding is the dominant driver of the exposure gradient, whereas micro-topographic protection (e.g., elevated floors) plays a secondary mitigating role at the city scale. Managerially, this pattern indicates that household-level elevation adjustments may reduce immediate nuisance impacts, but they cannot substitute for system-level flood-risk reduction when flood frequency remains high, particularly under compound flood conditions where coastal water levels and river discharge interact [44,53]. Accordingly, adaptation prioritization should differentiate “coping” measures (e.g., raising floors and temporary barriers) from interventions that reduce event frequency and duration (e.g., drainage upgrading, pump capacity, retention management, and corridor maintenance).

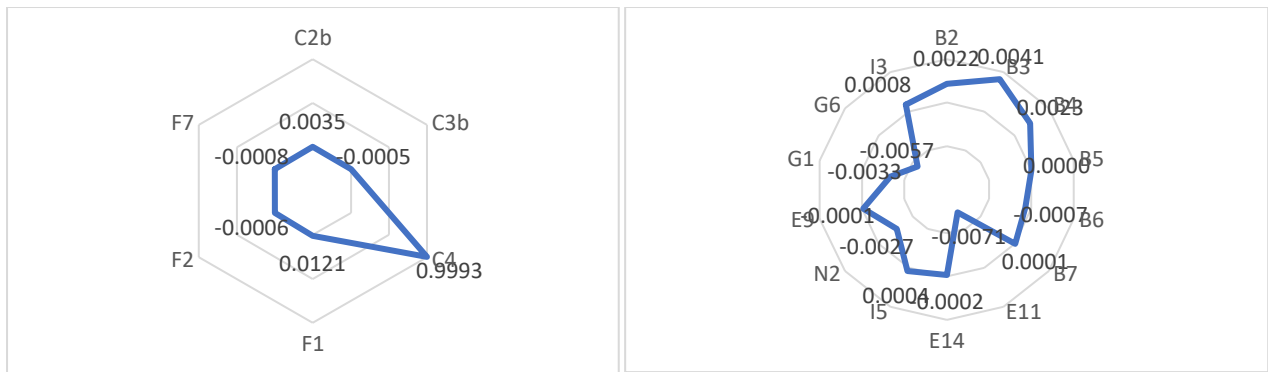


Figure 9. Exposure and sensitivity indicators and their variable loadings on the PC1. This figure presents the loading patterns of the variables included in the exposure and sensitivity dimensions on the first principal component, shown in two radar charts. The left panel displays exposure-related indicators, while the right panel shows sensitivity-related indicators, with each axis representing the loading value of an individual variable. The figure highlights the relative contribution of each variable to PC1 and helps identify the indicators that most strongly shape the resilience structure in the analysis.

Based on the results of the PCA for the sensitivity indicator, three main sectors contribute significantly: residence, health, and water sources. In the residential sector, the variable “building area (B3)” has the highest loading value of 0.0041, showing a negative relationship with household resilience. This indicates that the larger the building size, the lower the household’s resilience level, as larger houses are often located in densely populated or flood-prone areas. Thus, the physical characteristics of housing play an important role in determining household sensitivity to climate change impacts. In the health sector, the variable “Medical expenses after a disaster (E11)” showed the highest absolute loading value of -0.0071 , indicating a negative relationship with resilience. In other words, higher post-disaster medical expenditures are associated with lower household resilience, as financial burdens reduce the adaptive capacity. Conversely, households with a higher proportion of healthy family members after floods, droughts, or disease outbreaks, such as dengue fever, tend to demonstrate greater resilience. Meanwhile, in the water source sector, the variable “Source of drinking water (G6)” with a loading value of -0.0057 emphasizes that dependence on unsafe or unreliable water sources, especially after disasters, increases household sensitivity to health risks. Overall, family health conditions, housing quality, and access to clean water are key determinants of household sensitivity to the impacts of climate change in urban DKI Jakarta.

Sensitivity indicators should be interpreted as a household’s propensity to incur damage and welfare loss when hazards occur. In dense urban settings, sensitivity is often shaped by the reliability of basic services (safe water access and sanitation), housing materials/tenure security, and health constraints that limit response capacity. This is important because, even when exposure is similar, households with higher sensitivity can experience disproportionate losses, turning climate shocks into persistent welfare traps. Conceptually, this aligns with the socio-ecological resilience framing, where the robustness of core functions depends on both environmental stressors and the system’s internal fragilities [45].

Figure 10 presents the loading patterns of the incremental and transformational adaptation indicators on PC1, highlighting the variables that most strongly influence the resilience. The two variables with the highest loading values came from the economic and human resource sectors. In the economic sector, the variable “expenses per family member (A14)” had the highest loading value of 0.0282, showing a positive relationship with household resilience. This indicates that households with higher expenditures per family member tend to have greater adaptive capacity, as expenditure levels generally reflect household income and economic stability. Stronger financial capacity allows households to implement adaptive measures, such as improving home infrastructure, saving for emergencies, or purchasing equipment to enhance disaster preparedness.

The observed pattern that education and proactive behaviors relate to higher HCRI is consistent with the role of information access, risk perception, and planning capacity in enabling incremental adjustments (e.g., preparedness actions, routine maintenance, and early response). However, the contribution of these determinants should be discussed as “mechanisms”: education improves the ability to acquire and evaluate risk information, navigate assistance programs, and coordinate protective actions, especially when hazards are frequent and uncertainty is high [45]. Practically, this implies that adaptation programs should not only

disseminate information but also reduce transaction costs for uptake (clear eligibility, neighborhood-level facilitation, and repeated engagement), because incremental adaptation is often constrained by time, liquidity, and institutional access rather than awareness alone.



Figure 10. Incremental and transformational adaptation indicators and their variable loadings on the PC1. This figure presents the loading patterns of the variables included in the incremental and transformational adaptation dimensions on the first principal component, shown in two radar charts. The left panel displays incremental adaptation indicators, while the right panel shows transformational adaptation indicators, with each axis representing the loading value of an individual variable. The figure highlights the relative contribution of each variable to PC1 and helps identify the adaptation indicators that most strongly influence the resilience structure in the analysis.

Meanwhile, in the human resources sector, the variable “final education (A4)” has the highest loading value of 0.0059, also showing a positive relationship with resilience. Higher education levels of the household head are associated with better adaptive capacity, as education enhances knowledge, awareness, and decision-making ability in response to climate risks. Households with better-educated members are generally more proactive in implementing preventive measures, understanding early warning information, and engaging in community-based adaptation initiatives. Therefore, these two variables confirm that economic capacity and education are the main pillars shaping households’ incremental adaptive capacity to the impacts of climate change in DKI Jakarta.

Transformational adaptation indicators represent the household’s ability to make larger shifts, such as livelihood changes, relocation decisions, durable investments, and institutional connectedness. In a coastal megacity, these options are strongly mediated by governance and environmental systems (zoning enforcement, groundwater regulation, coastal protection planning), meaning that “transformational” capacity is partly a policy-produced opportunity set rather than only an individual attribute. This coupled framing strengthens the policy relevance of the HCRI: it can identify where households face chronic exposure yet lack feasible pathways to transform risk, pointing to areas where governance change is required, not merely household-level behavioral encouragement [46,54]. Based on the results of the PCA for the transformational adaptation indicator, the most influential variables come from the personal sector, particularly “flood adaptation efforts (D2)” and “number of people cleaning the house (E4.1)” which have the highest absolute loading values of -0.0072 and -0.0095 , respectively. Both variables showed a negative loading direction, but their interpretation aligned positively with household resilience, as higher engagement in adaptive and recovery activities indicated a stronger transformative capacity.

The variable “flood adaptation efforts (D2)” reflects proactive actions taken by households to mitigate the impacts of floods, such as building barriers, improving drainage, and relocating valuable goods during flood events. These activities represent a higher level of awareness and long-term adaptation, beyond reactive responses. Meanwhile, the “number of people cleaning the house (E4.1)” captures collective recovery behavior after disasters, where greater household participation in post-flood cleanup reflects stronger internal cooperation and resource mobilization, both of which enhance the adaptive capacity. Additionally, “drought adaptation efforts (J2)” with a loading value of -0.0032 also indicates households’ ability to adapt through efficient water use or alternative water sources. Overall, these findings emphasize that active participation, collective effort, and proactive adaptation measures are key components of transformational adaptation that strengthen household resilience to climate change impacts in DKI Jakarta.

Interpretation and Urban Environmental Management Implications

The north–south resilience gradient observed in Jakarta is consistent with patterns reported in other Indonesian coastal cities, where low-lying zones experience recurrent flooding and subsidence-amplified impacts. However, the governance and infrastructure context determine how hazards translate into household outcomes. For example, preparedness work in Semarang emphasizes that resilience is not only a matter of household capacity; it also depends on integrated risk assessment, land-use control in vulnerable zones, and coordinated stakeholder governance [21]. In DKI Jakarta, the hazard regime is intensified at the megacity scale: land subsidence, drainage/polder dependence, and compound coastal–river flooding can create chronic exposure that overwhelms incremental household coping, making system-level environmental management a first-order determinant of household resilience [3,43,55].

Comparative evidence from coastal megacities in Southeast Asia cautions that adaptation portfolios can become skewed toward “hard” measures and reactive responses when flooding is frequent and subsidence is ongoing. In such contexts, adaptation performance depends strongly on whether structural drivers, especially subsidence control, risk-informed land-use governance, and flood-system reliability, are addressed alongside household-level determinants (e.g., education and expenditure) [46,56]. For Jakarta, this implies a distributional interpretation: HCRI differences are not only about “who can adapt,” but also about “where governance and infrastructure enable adaptation to work,” and where they do not [3,57].

To make this interaction explicit, the Jakarta north–south gradient can be framed as a recurrent coastal-urban pattern in which place-based exposure dominates household coping when the hazard regime becomes chronic. Coastal/northern lowlands face compounded exposure (tidal flooding, subsidence-amplified inundation, and drainage backflow), whereas inland/southern zones typically experience less coastal compounding and, therefore, may benefit more from incremental household capacities. Accordingly, the manuscript should emphasize that the HCRI gradient reflects an interaction between household capacities and a locally produced hazard regime—an interaction that is strengthened or weakened by land-use control, groundwater governance, and flood-system performance [43,55,56].

The HCRI results can then be translated into concrete adaptation prioritization by mapping determinant–interventional linkages. Where low resilience is primarily driven by high flood frequency (exposure), the principal policy lever is system performance, such as drainage upgrading and maintenance, pump reliability, retention/pond management, and river–coastal interface management to reduce flood duration and recurrence [3]. Where low resilience is driven by sensitivity (housing quality, basic services, health, and water reliability), priority actions include upgrading service reliability and housing risk reduction in the most exposed neighborhoods [57]. Where low resilience reflects limited incremental and transformational adaptation capacity, interventions should reduce barriers to uptake through targeted support for preparedness investments, structured risk communication and clearer institutional access pathways. Crucially, subsidence control and groundwater governance are not merely “context,” but adaptation instruments that can shift the hazard regime faced by households. Therefore, they should be positioned explicitly as environmental management priorities, informed by the spatial distribution of the HCRI [43,55].

Methodologically, while conventional PCA can summarize dominant covariation patterns, it retains all indicators in each component, which can reduce interpretability and allow weakly contributing indicators to add to the noise. To address this limitation, the analysis can progress to Sparse PCA using elastic-net regularization, which combines L1 (lasso) and L2 (ridge) penalties to induce sparse loadings—filtering indicators that contribute minimally to PC1 and improving interpretability for policy translation [58,59]. In parallel, because urban resilience determinants are spatially heterogeneous, the roadmap naturally extends from global PCA to Geographically Weighted PCA, which estimates location-specific components and loadings [49]. Finally, because resilience indicator systems are vulnerable to multivariate outliers and leverage points, the robustification of local covariance estimation (e.g., MCD) is a logical next step [42] and can be further strengthened in high-dimensional or small-local-sample settings via regularized robust covariance determinant (MRCD) [29]. Taken together, these steps motivate a coherent forward path from Robust GWPCA [60] to Sparse GWPCA [61], and ultimately toward a Sparse–Robust GWPCA framework that simultaneously targets spatial heterogeneity, interpretability, and resistance to contamination.

Conclusions

This study confirms that climate change exacerbates environmental stress and socioeconomic vulnerability in coastal urban regions such as DKI Jakarta. By integrating robust statistical methods, this study successfully constructed a HCRI that captures multidimensional resilience through indicators of exposure, sensitivity, and adaptive capacity. The application of RPCA MCD enhances the estimation stability in heterogeneous and outlier-prone data, enabling a more reliable resilience assessment. The results reveal pronounced spatial disparities, with northern coastal districts consistently exhibiting low resilience owing to recurrent flooding, tidal inundation, and limited adaptive capacity, whereas southern and central areas demonstrate stronger socio-economic and infrastructural resilience. Key factors that enhance resilience include education, economic capacity, and proactive adaptation behaviors. The clear north–south gradient highlights the importance of localized assessment approaches to account for spatial heterogeneity in resilience determinants. Overall, the HCRI framework developed in this study provides a robust empirical foundation for evidence-based urban climate adaptation policies and contributes to the achievement of SDG 11 (sustainable cities and communities) and SDG 13 (climate action) in Indonesia’s rapidly urbanizing context.

Author Contributions

MS: Conceptualization, Methodology, Software, Investigation, Writing – Review & Editing; **KS:** Conceptualization, Methodology, Investigation, Writing – Review, Supervision; **AHW:** Conceptualization, Methodology, Investigation, Review – Supervision, **AF:** Conceptualization, Methodology, Investigation, Writing – Review, Supervision, and **RB:** Conceptualization, Methodology, Investigation, Writing – Review, Supervision.

AI Writing Statement

During the preparation of this work, the author used ChatGPT (OpenAI) to improve the clarity of academic writing and refine non-substantive descriptions of methods and code comments. After using this tool/service, the author reviewed and edited the content as needed and takes full responsibility for the content of the publication.

Conflicts of interest

There are no conflicts to declare.

Acknowledgments

We are grateful to the Center for Climate Risk and Opportunity Management in Southeast Asia and the Pacific (CCROM-SEAP), Bogor Agricultural University, and the Environmental Agency (DLH) of Jakarta for their collaboration and unwavering support in this research. Their essential role in providing data, conducting analyses, and sharing profound insights was vital to the progress of this study. This research was supported by the Directorate General of Research and Development, Ministry of Higher Education, Science, and Technology under the Research Program Implementation Contract for Fiscal Year 2025, No. 006/C3/DT.05.00/PL/2025.

References

1. Fazey, I.; Carmen, E.; Chapin, F.S.; Ross, H.; Rao-Williams, J.; Lyon, C.; Connon, I.L.C.; Searle, B.A.; Knox, K. Community Resilience for a 1.5°C World. *Curr. Opin. Environ. Sustain.* **2018**, *31*, 30–40, doi:<https://doi.org/10.1016/j.cosust.2017.12.006>.
2. Lanlan, J.; Sarker, M.N.I.; Ali, I.; Firdaus, R.B.R.; Hossin, M.A. Vulnerability and Resilience in the Context of Natural Hazards: A Critical Conceptual Analysis. *Environ. Dev. Sustain.* **2024**, *26*, 19069–19092, doi:[10.1007/s10668-023-03440-5](https://doi.org/10.1007/s10668-023-03440-5).
3. IPCC (Intergovernmental Panel on Climate Change). Summary for policymakers. In *Climate Change 2022: Impacts, Adaptation and Vulnerability*; Pörtner, H.-O., Roberts, D.C., Tignor, M., Poloczanska, E.S.,

- Mintenbeck, K., Alegría, A., Craig, M., Langsdorf, S., Löschke, S., Möller, V., et al., Eds.; Cambridge University Press: Cambridge, UK, and New York, USA, 2022; pp. 3–34, ISBN 9781009325837.
4. IPCC (Intergovernmental Panel on Climate Change). Summary for policymakers. In *Climate Change 2023: Synthesis Report*; Lee, H., Romero, J., Eds.; IPCC: Geneva, Switzerland, 2023; pp. 1–34.
 5. Schipper, E.L.F.; Revi, A.; Preston, B.L.; Carr, E.R.; Eriksen, S.H.; Fernandez-Carril, L.R.; Glavovic, B.; Hilmi, N.J.M.; Ley, D.; Mukerji, R.; et al. Climate Resilient Development Pathways. In *Climate Change 2022: Impacts, Adaptation, and Vulnerability*; Cambridge University Press: Cambridge, UK, 2022; pp. 2655–2807, ISBN 0521775728.
 6. UNDRR (United Nations Office for Disaster Risk Reduction). *Global Assessment Report on Disaster Risk Reduction 2022: Our World at Risk: Transforming Governance for a Resilient Future*; UNDRR: Geneva, Switzerland, 2022; ISBN 9789212320281.
 7. Ferrario, F.; Mourato, J.M.; Rodrigues, M.S.; Dias, L.F. Evaluating Nature-Based Solutions as Urban Resilience and Climate Adaptation Tools: A Meta-Analysis of Their Benefits on Heatwaves and Floods. *Sci. Total Environ.* **2024**, *950*, 175179, doi:<https://doi.org/10.1016/j.scitotenv.2024.175179>.
 8. Mosisa, G.; Bedadi, B.; Dale, G.; Abate, N.T. Nature-Based Solutions for Urban Climate Resilience: Implementation, Contribution, and Effectiveness. *Nature-Based Solut.* **2025**, *8*, 100245, doi:[10.1016/j.nbsj.2025.100245](https://doi.org/10.1016/j.nbsj.2025.100245).
 9. Suárez, M.; Benayas, J.; Justel, A.; Sisto, R.; Montes, C.; Sanz-Casado, E. A Holistic Index-Based Framework to Assess Urban Resilience: Application to the Madrid Region, Spain. *Ecol. Indic.* **2024**, *166*, 112293, doi:<https://doi.org/10.1016/j.ecolind.2024.112293>.
 10. Cheng, Y.; Si, H.; Bao, Z. Evaluating Megacity Resilience to Pandemics: The Case of China. *Risk Anal.* **2025**, *45*, 3626–3642, doi:[10.1111/risa.70102](https://doi.org/10.1111/risa.70102).
 11. Khan, M.A. Vision of a sustainable, smart, and resilient city. In *Cities and Mega Risks: COVID-19 and Climate Change*; Springer: Cham, Switzerland, 2022; pp. 295–338, ISBN 978-3-031-14087-7.
 12. Adger, W.N.; Brown, K.; Nelson, D.R.; Berkes, F.; Eakin, H.; Folke, C.; Galvin, K.; Gunderson, L.; Goulden, M.; O'Brien, K. Resilience Implications of Policy Responses to Climate Change. *Wiley Interdiscip. Rev. Clim. Chang.* **2011**, *2*, 757–766.
 13. Patel, N.; Jänicke, B.; Burghardt, R.; Vulova, S.; Otto, F. Assessing Progress in Urban Climate Adaptation: A Review of Indicators for Heat- and Water-Sensitive Urban Development. *Clim. Resil. Sustain.* **2025**, *4*, e70009, doi:[10.1002/cli2.70009](https://doi.org/10.1002/cli2.70009).
 14. Pellerey, V.; Moghadam, S.T.; Lombardi, P. A Systematic Review of Justice Integration to Climate Resilience: Current Trends and Future Directions. *Urban Clim.* **2025**, *59*, 102250, doi:<https://doi.org/10.1016/j.uclim.2024.102250>.
 15. Akter, M.M.; Hosen, M.I.; Nasher, N.M.R. Assessing Household Resilience to Climate Extremes Using Indicator-Based Index in Hazard-Prone Areas; Evidence from Bangladesh. *Environ. Challenges* **2024**, *15*, 100957, doi:<https://doi.org/10.1016/j.envc.2024.100957>.
 16. Yessoufou, A.N.-D.; Kumar, S.; Houessionon, P.; Worou, O.N.; Wane, A.; Whitbread, A. Vulnerability and Resilience in the Face of Climate Changes in Senegal's Drylands: Measurement at the Household Level and Determinant Assessment. *Front. Clim.* **2024**, *6*, 1330025, doi:[10.3389/fclim.2024.1330025](https://doi.org/10.3389/fclim.2024.1330025).
 17. BPBD (Badan Penanggulangan Bencana Daerah). *Infografis Kejadian Bencana Provinsi DKI Jakarta Tahun 2021*; BPBD: Jakarta, ID, 2021;
 18. Dinas Lingkungan Hidup Provinsi DKI Jakarta. *Pelaksanaan Adaptasi Dalam Rangka Memperkuat Ketahanan Iklim Provinsi DKI Jakarta*; Dinas Lingkungan Hidup Provinsi DKI Jakarta: Jakarta, ID, 2021;
 19. Iskandar, A.; Makarim, C.A.; Chandra, T.K. Studi Kasus Penurunan Muka Tanah dan Muka Air Tanah Di Jakarta Pusat Tahun 2010-2022. *JMTS J. Mitra Tek. Sipil* **2025**, *8*, 549–558.
 20. Simon, M. Jakarta Is Sinking. Now Indonesia Has to Find a New Capital. *Wired*, 2 May 2019. Available online: <https://www.wired.com/story/jakarta-is-sinking/> (accessed on 8 September 2025).
 21. Hayati, R.; Findayani, A.; Amrullah, M.F. CDRI (Climate Disaster Resilience Index) for Analysis of Semarang City's Resilience to Climate Change Disasters. *IOP Conf. Ser. Earth Environ. Sci.* **2025**, *1479*, 12062.

22. Asmamaw, M.; Mereta, S.T.; Ambelu, A. Exploring Households' Resilience to Climate Change-Induced Shocks Using Climate Resilience Index in Dinki Watershed, Central Highlands of Ethiopia. *PLoS One* **2019**, *14*, e0219393.
23. Shah, K.U.; Dulal, H.B.; Johnson, C.; Baptiste, A. Understanding Livelihood Vulnerability to Climate Change: Applying the Livelihood Vulnerability Index in Trinidad and Tobago. *Geoforum* **2013**, *47*, 125–137, doi:<https://doi.org/10.1016/j.geoforum.2013.04.004>.
24. Hubert, M.; Debruyne, M.; Rousseeuw, P.J. Minimum Covariance Determinant and Extensions. *WIREs Comput. Stat.* **2018**, *10*, e1421, doi:10.1002/wics.1421.
25. Jolliffe, I.T.; Cadima, J. Principal Component Analysis: A Review and Recent Developments. *Philos. Trans. Ser. A, Math. Phys. Eng. Sci.* **2016**, *374*, 20150202, doi:10.1098/rsta.2015.0202.
26. Rousseeuw, P.J.; van Zomeren, B.C. Unmasking Multivariate Outliers and Leverage Points. *J. Am. Stat. Assoc.* **1990**, *85*, 633–639.
27. Subiyanto, A.; Boer, R.; Aldrian, E.; Kinseng, R. Climate Resilience: Concepts, Theory and Methods of Measuring. *EnvironmentAsia* **2020**, *13*, 1–13.
28. Skondras, N.A.; Tsemelis, D.E.; Vasilakou, C.G.; Karavitis, C.A. Resilience–Vulnerability Analysis: A Decision-Making Framework for Systems Assessment. *Sustainability* **2020**, *12*, 1–14.
29. Boudt, K.; Rousseeuw, P.J.; Vanduffel, S.; Verdonck, T. The Minimum Regularized Covariance Determinant Estimator. *Stat. Comput.* **2020**, *30*, 113–128.
30. Maronna, R.A.; Martin, R.D.; Yohai, V.J.; Salibián-Barrera, M. *Robust Statistics: Theory and Methods (with R)*; John Wiley & Sons: West Sussex, UK, 2019; ISBN 1119214688.
31. Bappeda (Badan Perencanaan Pembangunan Daerah) Jakarta. *RPJMD DKI Jakarta 2017–2022*; Pemerintah Provinsi DKI Jakarta: Jakarta, ID, 2018;
32. BPS (Badan Pusat Statistik) Jakarta. *DKI Jakarta Dalam Angka 2022*; BPS: Jakarta, ID, 2022;
33. Boer, R.; Dasanto, B.D.; Wijayanti, P.; Jadmiko, S.D.; Rafuddin, A.; Anggraeni, L.; Hidayati, R. *Kajian Dampak Perubahan Iklim Terhadap Lingkungan, Sosial, Ekonomi Dan Kesehatan di Provinsi DKI Jakarta*; IPB University: Bogor, ID, 2022;
34. Green, B. The method of successive intervals: a sourcebook for behavioral scientists. In *Scaling: A Sourcebook for Behavioral Scientists*; Routledge: New York, USA, 2017; pp. 122–128, ISBN 9781315128948.
35. Todorov, V.; Filzmoser, P. An Object-Oriented Framework for Robust Multivariate Analysis. *J. Stat. Softw.* **2009**, *32*, 1–47, doi:10.18637/jss.v032.i03.
36. IPCC (Intergovernmental Panel on Climate Change). Summary for policymakers. In *Climate Change 2014: Impacts, Adaptation, and Vulnerability. Part A: Global and Sectoral Aspects*; Field, C.B., Barros, V.R., Dokken, D.J., Mach, K.J., Mastrandrea, M.D., Bilir, T.E., Chatterjee, M., Ebi, K.L., Estrada, Y.O., Genova, R.C., et al., Eds.; Cambridge University Press: Cambridge, UK and New York, USA, 2014; ISBN 978-1-107-05807-1.
37. Subiyanto, A. *Ketahanan Nasional Dan Resiliensi Iklim*; CV. PenerbitQjara Media: Pasuruan, Indonesia, 2021; ISBN: 978-623-555-176-0.
38. Jolliffe, I.T. *Principal Component Analysis*, 2nd ed.; Springer: New York, USA, 2002;
39. ATSDR (Agency for Toxic Substances and Disease Registry). Social Vulnerability Index. 2024. Available online: https://www.atsdr.cdc.gov/place-health/php/svi/index.html#:~:text=The Centers for Disease Control and Prevention, Loss of property * Illness * Death (accessed on 2 February 2026).
40. Zhao, Y.; Paul, R.; Reid, S.; Vieira, C.C.; Wolfe, C.; Zhang, Y.; Chunara, R. Constructing Social Vulnerability Indexes with Increased Data and Machine Learning Highlight the Importance of Wealth across Global Contexts. *Soc. Indic. Res.* **2024**, *175*, 639–657.
41. UNISDR (United Nations Office for Disaster Risk Reduction). Sendai Framework for Disaster Risk Reduction 2015–2030. 2015. Available online: <https://www.undrr.org/media/16176/download?startDownload=20260313> (accessed on 12 March 2026).
42. Rousseeuw, P.J.; Van Driessen, K. A Fast Algorithm for the Minimum Covariance Determinant Estimator. *Technometrics* **1999**, *41*, 212–223.

43. Abidin, H.Z.; Andreas, H.; Gumilar, I.; Fukuda, Y.; Pohan, Y.E.; Deguchi, T. Land Subsidence of Jakarta (Indonesia) and Its Relation with Urban Development. *Nat. hazards* **2011**, *59*, 1753–1771.
44. Bennett, W.G.; Karunarathna, H.; Xuan, Y.; Kusuma, M.S.B.; Farid, M.; Kuntoro, A.A.; Rahayu, H.P.; Kombaitan, B.; Septiadi, D.; Kesuma, T.N.A. Modelling Compound Flooding: A Case Study from Jakarta, Indonesia. *Nat. Hazards* **2023**, *118*, 277–305.
45. Meerow, S.; Newell, J.P.; Stults, M. Defining Urban Resilience: A Review. *Landscape and Urban Planning* **2016**, *147*, 38–49.
46. Scheiber, L.; David, C.G.; Jalloul, M.H.; Visscher, J.; Nguyen, H.Q.; Leitold, R.; Revilla Diez, J.; Schlurmann, T. Low-Regret Climate Change Adaptation in Coastal Megacities—Evaluating Large-Scale Flood Protection and Small-Scale Rainwater Detention Measures for Ho Chi Minh City, Vietnam. *Nat. Hazards Earth Syst. Sci.* **2023**, *23*, 2333–2347.
47. Matandirotya, N.R.; Filho, W.L.; Mahed, G.; Dinis, M.A.P.; Mathe, P. Local Knowledge of Climate Change Adaptation Strategies from the VhaVenda and BaTonga Communities Living in the Limpopo and Zambezi River Basins, Southern Africa. *Inl. Waters* **2024**, *14*, 268–280, doi:10.1080/20442041.2024.2437932.
48. Lu, B.; Hu, Y.; Yang, D.; Liu, Y.; Ou, G.; Harris, P.; Brunsdon, C.; Comber, A.; Dong, G. GWmodelS: A Standalone Software to Train Geographically Weighted Models. *Geo-spatial Inf. Sci.* **2025**, *28*, 648–670, doi:10.1080/10095020.2024.2343011.
49. Harris, P.; Brunsdon, C.; Charlton, M. Geographically Weighted Principal Components Analysis. *Int. J. Geogr. Inf. Sci.* **2011**, *25*, 1717–1736.
50. Aidoo, E.N.; Appiah, S.K.; Awashie, G.E.; Boateng, A.; Darko, G. Geographically Weighted Principal Component Analysis for Characterising the Spatial Heterogeneity and Connectivity of Soil Heavy Metals in Kumasi, Ghana. *Heliyon* **2021**, *7*, e08039, doi:10.1016/j.heliyon.2021.e08039.
51. Palma, M.; De Iaco, S.; Cappello, C.; Distefano, V. Tourism Composite Spatial Indicators through Variography and Geographically Weighted Principal Components Analysis. *Ann. Oper. Res.* **2024**, *342*, 1687–1705, doi:10.1007/s10479-023-05329-y.
52. Zardo, L.; Cortinovis, C.; Lucertini, G. Prejudices May Be Wrong: Exploring Spatial Patterns of Vulnerability to Energy Poverty in Italian Metropolitan Areas. *Sustainability* **2024**, *16*, 1–18.
53. Duy, P.N.; Chapman, L.; Tight, M.; Thuong, L. V; Linh, P.N. Urban Resilience to Floods in Coastal Cities: Challenges and Opportunities for Ho Chi Minh City and Other Emerging Cities in Southeast Asia. *J. Urban Plan. Dev.* **2018**, *144*, 5017018.
54. Prianda, B.G.; Widodo, E. Perbandingan Metode Seasonal Arima Dan Extreme Learning Machine Pada Peramalan Jumlah Wisatawan Mancanegara Ke Bali. *Barekeng J. Ilmu Mat. dan Terap.* **2021**, *15*, 639–650, doi:10.30598/barekengvol15iss4pp639-650.
55. Handika, R.; Widodo, J.; Pravitasari, A.E. Combined Land Subsidence Analysis in Jakarta Based on Ps-InSAR and MICMAC Methods. *J. Teknol. Lingkungan.* **2024**, *25*, 137–145.
56. Siriwardane-de Zoysa, R.; Schöne, T.; Herbeck, J.; Illigner, J.; Haghighi, M.; Simarmata, H.; Porio, E.; Rovere, A.; Hornidge, A.-K. The ‘Wickedness’ of Governing Land Subsidence: Policy Perspectives from Urban Southeast Asia. *PLoS One* **2021**, *16*, e0250208.
57. Dwirahmadi, F.; Barnes, P.; Wibowo, A.; Amri, A.; Chu, C. Linking Disaster Risk Reduction and Climate Change Adaptation through Collaborative Governance: Experience from Urban Flooding in Jakarta. *Geosciences* **2023**, *13*, 1–14.
58. Zou, H.; Hastie, T. Regularization and Variable Selection via the Elastic Net. *J. R. Stat. Soc. Ser. B: Statistical Methodol.* **2005**, *67*, 301–320.
59. Zou, H.; Hastie, T.; Tibshirani, R. Sparse Principal Component Analysis. *J. Comput. Graph. Stat.* **2006**, *15*, 265–286.
60. Harris, P.; Brunsdon, C.; Charlton, M.; Juggins, S.; Clarke, A. Multivariate Spatial Outlier Detection Using Robust Geographically Weighted Methods. *Math. Geosci.* **2014**, *46*, 1–31.
61. Hong, S.-Y.; Moon, S.; Chi, S.-H.; Cho, Y.-J.; Kang, J.-Y. Local Sparse Principal Component Analysis for Exploring the Spatial Distribution of Social Infrastructure. *Land* **2022**, *11*, 1–16.